

Transferring Noncharring Polyolefins to Charring Polymers with the Presence of Mo/Mg/Ni/O Catalysts and the Application in Flame Retardancy

Rongjun Song, Yao Fu, Bin Li

Heilongjiang Key Laboratory of Molecular Design and Preparation of Flame Retarded Materials, College of Science, Northeast Forestry University, Harbin 150040, People's Republic of China

Correspondence to: R. Song (E-mail: rongjunsong@nefu.edu.cn)

ABSTRACT: This article presents a novel investigation on the Mo/Mg/Ni/O catalysts (Nmm-cats) with which the noncharring polyolefins are basically transferred to the charring polymers under forced flaming conditions and the flame retardancy of polyolefins is improved dramatically. The results of model charring experiments show that when appropriate Mo/Mg/Ni molar ratio is adopted and only 3% Nmm-cats is blended, the Nmm-cats belong to high-efficient charring catalysts that can deposit 56 and 64 wt % of volatile products in-situ from linear low-density polyethylene (LLDPE) and polypropylene (PP), respectively. The charring properties are characterized by scanning electron microscopy, transmission electron microscopy, and Raman spectroscopy; and the char-forming mechanisms are analyzed by wide-angle X-ray diffraction experiment. The improvement in flammability properties for LLDPE and PP is demonstrated by using a cone calorimeter. © 2012 Wiley Periodicals, Inc. *J. Appl. Polym. Sci.* 129: 138–144, 2013

KEYWORDS: flame retardance; degradation; polyolefins

Received 26 June 2012; accepted 13 October 2012; published online 3 November 2012

DOI: 10.1002/app.38717

INTRODUCTION

The polyolefins, such as polyethylene (PE) and polypropylene (PP), are widely applied in commodities, indoor fitments, automobile industry, electric products, medical field, etc. They are presently the fastest growing synthetic polymers for their high tensile strength coupling with low cost.^{1–1} However, the inherent flammability has recently hindered their usages for safety considerations. Because of their whole aliphatic hydrocarbon structures, the polyolefin thermoplastics by themselves burn very rapidly with a relatively smoke-free flame and without leaving any carbonaceous residues. It is a real challenge to find an environmental friendly and high-efficient flame retardant for them due to no reactive side chains exist in their structures which can prevent charring formation following elimination of these groups in the condensed phase. As far as I know, almost no flame retardants used in polyolefins can deposit most aliphatic degradation products as char residues during combustion so far.

Numerous literatures have identified that Fe, Co, and Ni metal compounds possess the catalyzing and carbonizing capabilities for hydrocarbons under high temperature conditions.^{4–4} As we all know, the catalytic activity of Ni catalysts is the highest, but their lifetime is very short due to easy formation of amorphous carbon coating on their surfaces. This phenomenon was

confirmed when carbon nanotubes (CNT) were synthesized, where H₂ was often introduced together with carbon source to remove the amorphous carbon for increasing the lifetime of Ni catalysts.^{9–9} At recent reports, Hata et al. found that water acted in preserving the catalytic activity as a result of selectively removing the amorphous carbon at growth temperatures.^{12,13} We previously attempted to keep the catalytic activity of Ni catalysts blended into PP matrix by adding some synergistic agents. The results showed that the presence of organoclays, acidic zeolites or some halogenated compounds could preserve the activity of supported Ni(0) or Ni₂O₃ catalysts and deposit larger amount of volatile compounds during PP combustion.^{14–14} These two-component charring agents (Ni catalysts and synergistic additives) have a very important value for theoretical study due to their high capacity in carbonizing the gas-phase degradation products, However, the catalytic efficiency of them is still low owing to the separation of the two components in PP matrix.

In the present work, we prepared a single charring catalyst that could effectively scavenge alkyl radicals by catalytic carbonization in gas phase and then form a carbonaceous layer at the surface of polyolefins. The carbonaceous layer possessed the barrier function which could inhibit further degradation in the

condensed phase. We found that the Mo and Mg elements acted in promoting and preserving the catalytic activity of Ni catalysts. Recently, the Mo/Mg/Ni/O catalysts have been reported as catalysts to produce CNTs in hydrocarbon chemical vapor deposition (CVD) methods.^{19,20} However, to our best knowledge, there have previously been no such reports on the use of them as charring catalysts for the polyolefins. It has been demonstrated in the field of CNT synthesis that the combination of Mg and Mo elements could induce an increased effect on the activity of Ni catalysts. Nevertheless, as we incorporated these Mo/Mg/Ni/O catalysts into the polyolefin matrix, a very low yield of carbonaceous residues was left and there was a very weak effect on the flammability reduction of the polyolefin materials. It was reasonably explained that over-high levels of Mo and Mg elements largely decreased the molar fractions of Ni catalysts in the Mo/Mg/Ni/O catalysts and finally resulted in the reduction of charring efficiency. Therefore, we have to prepare a new type of Mo/Mg/Ni/O catalysts with high char-forming performance under polyolefin combustion conditions.

EXPERIMENTAL

Materials and Preparation of Samples

The Mo/Mg/Ni/O catalysts were prepared by combustion basing on two previous works.²¹ An amount of analytically pure $\text{Mg}(\text{NO}_3)_2 \cdot 6\text{H}_2\text{O}$, $(\text{NH}_3)_6\text{Mo}_7\text{O}_{24} \cdot 4\text{H}_2\text{O}$, and $\text{Ni}(\text{NO}_3)_2 \cdot 6\text{H}_2\text{O}$ were dissolved in PEG200. The solution was subsequently placed in a muffle heated at 650°C. It immediately ignited, and the fire lasted for 5 min. After the fire went out, the formed material was kept at 650°C for an additional 5 min. Finally, the product was obtained and ground to fine powders. The linear low-density polyethylene (LLDPE, melt flow index of 2.4 g/min) and PP (melt flow index of 0.8 g/min) were selected as two model polyolefins which were purchased from Jilin Petrochemical Co. The obtained catalysts were blended into the LLDPE and PP in a Brabendermixer at 100 rpm at 165 and 180°C for 10 min. The blended composites were molded with a press-type molding machine to make the required shape.

Characterization

The charring test was performed by a pyrolyzer that was heated to 700°C in an N_2 atmosphere. About 10 g of the above LLDPE/catalysts or PP/catalysts composites were put into the pyrolyzer and kept heating until no gaseous released, and then the residues were collected. The amount of charred residues was obtained by subtracting the amount of catalysts. The char yield was calculated by amount of the charred residues divided by amount of polymers used in the sample, i.e., $y = (M/M_{\text{PO}}) \times 100\%$; the weight ratio of polyolefin/catalysts was 97/3.

Flammability of the composites was determined by a cone calorimeter (Fire Testing Technology, East Grinstead, UK) tests which was performed according to ISO5660 standard, namely at a heat flux of 50 kW/m², 1.24 L/s of exhaust flow rate and the spark was continuous until the sample was ignited. The specimens to be tested in the cone calorimeter were prepared by the compression molding of the sample into 6 × 100 × 100 mm³ square plaques. The LOI value was measured on a JF-3 oxygen index meter (Jiangning, China) with sheet dimensions of 130 × 6.5 × 3 mm³, according to ISO4589-1984.

Table I. Relationship Between the Char Yield with the Addition of Mg and Mo Elements in the Ni Catalysts

| | Mo/Mg/Ni (mole ratio) | Char yield (%) |
|------|-----------------------|----------------|
| CA0 | 1/7 | 5 |
| CA1 | 1/0.25/7 | 9 |
| CA2 | 1/0.5/7 | 12 |
| CA3 | 1/1.0/7 | 16 |
| CA4 | 1/1.25/7 | 11 |
| CA5 | 0.42/1/7 | 21 |
| CA6 | 0.7/1/7 | 34 |
| CA7 | 1.05/1/7 | 30 |
| CA8 | 0.21/1.0/7 | 39 |
| CA9 | 0.42/1.0/7 | 46 |
| CA10 | 0.7/1.0/7 | 56 |
| CA11 | 1.05/1.0/7 | 43 |
| CA12 | 1.4/1.0/7 | 38 |

The morphologies of the carbonaceous residues were examined with field-emission scanning electron microscopy (FE-SEM, XL303SEM) and transmission electron microscopy (TEM, JEM-2010); Raman spectroscopy (T6400, excitation-beam wavelength: 514.5 nm) was used to characterize the vibrational properties of the obtained char materials. Wide-angle X-ray diffraction experiment was also performed for the catalysts and the corresponding obtained carbonaceous residues by using a Rigaku D/MAX-IIB powder X-ray diffractometer with CuK α radiation ($\lambda = 1.54 \text{ \AA}$).

RESULTS AND DISCUSSION

To validate the hypothesis that the Ni catalysts with the presence of appropriate contents of Mo and Mg elements could effectively carbonize the degradation products of polyolefins under high-temperature conditions, we performed a model charring measurement on the samples for which 3 wt % of catalysts were blended in a typical polyolefin polymer, LLDPE. As Ni element is the requisite constituent in the Mo/Mg/Ni/O catalysts, we first investigate the effect of the incorporation of Mg elements on the charring capacity of Ni catalysts. As listed in Table I, the char yield increases monotonically with the increase of the molar fraction of Mg element in Mg/Ni/O catalysts until the Mg/Ni molar ratio achieves 1/7, the corresponding charring yield is 16%. However, further increasing the molar fraction of Mg induces a negative effect on the yield of charring. In addition, the influence of Mo element on the charring performance of Ni catalysts was likewise studied for the LLDPE matrix. After comparing the synergistic effect provided by Mg element, it is found that the incorporation of Mo element in Ni catalysts is more effective to enhance the char yield as listed in Table I. It is similar with the effect of Mg element, the char yield decreases at much higher Mo contents.

Owing to the difference in synergistic effects between Mo and Mg elements, we subsequently examined the effect of the coexistence of Mg and Mo elements in Ni catalysts on the char yield of LLDPE/catalyst composites. Surprisingly, the coexistence of

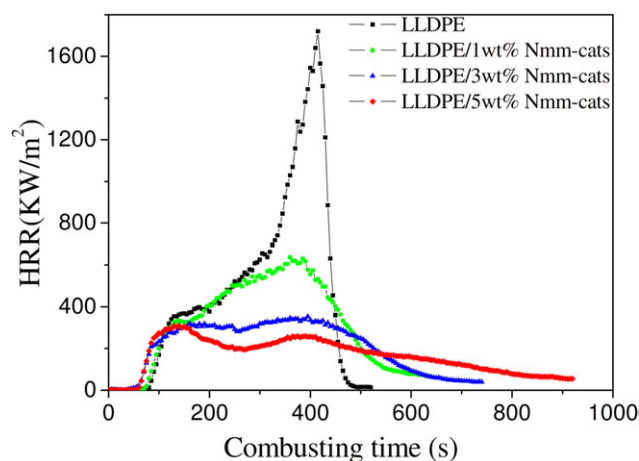


Figure 1. Effects of the mass fraction of Nmm-cats on the heat release rate of LLDPE/Nmm-cats. [Color figure can be viewed in the online issue, which is available at wileyonlinelibrary.com.]

Mg and Mo elements in Ni catalysts significantly promotes the formation of char, and the highest char yield (56%) is obtained when the Mo/Mg/Ni molar ratio is 0.7/1/7 (Table I). Thus, we have demonstrated that for the Ni catalysts, when an appropriate concentration of Mo and Mg elements were combined, the composite catalysts had a highly increased efficiency in depositing the gas-phase degradation products of LLDPE under high temperature conditions. Compared with our previous results in the presence of double fillers, the char yield was increased by more than two times with the same 3 wt % loadings in LLDPE. In a word, we have completely transferred the noncharring LLDPE to a charring polymer by depositing most of the gas degradation products with very low levels of fillers in the LLDPE matrix. Henceforth, we name the Mo/Mg/Ni/O catalyst with the molar ratio of 0.7/1/7 as the Nmm-cats owing to its highest charring performance in LLDPE matrix.

Formation of the carbonaceous materials from LLDPE itself during combustion could act as a heat shield for the unburned polymer below them, thus the cone calorimeter measurement was performed to determine the effect of the addition of Nmm-cats on the flame retardancy of LLDPE. Results of the cone experiments with various concentrations of Nmm-cats are reported in Figure 1 and Table II. The heat release rate (HRR) and the total heat release (THR) of the pure LLDPE are the highest among the four samples due to their noncharring properties, whereas all the samples show almost the same ignition time (IT). The region surrounded by the HRR curve seems to be a steep mountain with a very high mountain peak (1720 kW/m²) and a relative small span length of 400 s, which indicates that the pure LLDPE has a very short combusting time and a very high peak heat release rate (PHRR) which is a key flammability measure in the force combustion. As confirmed in Table I, the gas-phase degradation products of LLDPE can be carbonized catalytically by the incorporated Nmm-cats during combustion. Thus we expect that the presence of Nmm-cats can result in a significant reduction in HRR. Indeed, as shown in Figure 1 and Table II, the PHRR of LLDPE is strongly reduced even when the Nmm-cat mass fraction is as low as 1%. At the same

time, a decreased THR (216 MJ/m²) and an appeared char yield (22%) was measured from the cone experiments after 600 s. When the mass fraction of Nmm-cats was increased to 3 wt %, a far more decreased PHRR (340 kW/m²) and THR (187 MJ/m²) were observed owing to much more char formed from the samples, as confirmed in Table II. However, this trend did not continue when the Nmm-cat mass fraction was further increased to 5 wt %. Compared with the LLDPE/3 wt % Nmm-cats, the PHRR value of LLDPE/5 wt % Nmm-cats appeared at about 140 s does not show appreciable reduction, which indicates that 3 wt % Nmm-cat addition in LLDPE is sufficient to form a carbonaceous layer and effectively protect the below polymers from further accelerating degradation. Differently, however, the LLDPE/5 wt % Nmm-cats has a much lower HRR curve compared with that of the LLDPE/3 wt % Nmm-cats after the PHRR point. It meant that more gas-phase degradation products have been deposited in the case of LLDPE/5 wt % Nmm-cats; indeed, from Table II, it is clearly seen that more amounts of char residues have been formed from LLDPE/5 wt % Nmm-cats than those from LLDPE/3 wt % Nmm-cats. In addition, a comparison was made between the char yield of LLDPE/3 wt % Nmm-cats in the cone experiments as listed in Table II and the model charring test in Table I. It shows that the char yield achieved in the cone experiments is relatively low. In present work, we believe that the char yield reduction is due to the different heat flux conditions and the partial oxidation even after flame out in the cone measurements, and it has no correlation with the different atmosphere used for both experiments. On the other hand, since the char depositing has influenced the flammability of volatiles produced from LLDPE during burning, the average EHC decreases gradually with the increase of Nmm-cat contents (Table II).

To further demonstrate the catalytic carbonization performance of the Nmm-cats for the gas-phase degradation products of LLDPE, a relatively thick sample with 5% mass fraction of Nmm-cats was selected to provide a video image of intermediate morphologies by interrupting the process of cone measurement. Figure 2 shows that a thick layer of carbonaceous substances has been formed at the surface of the sample rather than a thin layer with some supporting frames formed from some polymer nanocomposites reported in some literatures.^{22–23} Therefore it provides a more effective protection for the LLDPE

Table II. Cone Calorimeter and LOI Data of LLDPE and LLDPE/Nmm-Cat Composites

| Properties | LLDPE | LLDPE/1% Nmm-cat | LLDPE/3% Nmm-cat | LLDPE/5% Nmm-cat |
|---------------------------|-------|------------------|------------------|------------------|
| IT(s) | 69 | 69 | 66 | 65 |
| PHRR (kW/m ²) | 1720 | 637 | 339 | 330 |
| THR (MJ/m ²) | 245.7 | 216 | 187 | 154 |
| Average EHC (MJ/Kg) | 38.6 | 38.2 | 36.7 | 36.2 |
| Char yield (%) | 0 | 22 | 43 | 55 |
| LOI (%) | 17.2 | 17.2 | 18 | 18.5 |

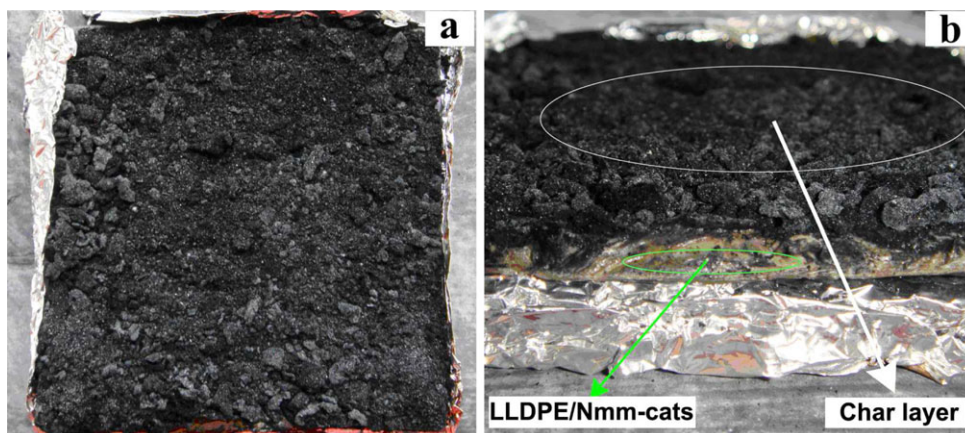


Figure 2. Video images of LLDPE/5 wt % Nmm-cats sample at intermediary stage in cone calorimeter. [Color figure can be viewed in the online issue, which is available at wileyonlinelibrary.com.]

matrix under it. Indeed, when we stripped off the covering of aluminum foil, the unburned LLDPE/Nmm-cats composites were clearly observed and seemed to be an intact sample without any exposure to the external radiant flux in Figure 2(b). These observations provide a direct evidence for the high charring effectiveness and the perfect flame-retardant performance of the Nmm-cats for LLDPE.

To completely examine the flame-retardant performance of the Nmm-cats for LLDPE, the LOI test was performed on the samples for a range of Nmm-cat concentrations. It was found that the surfaces of the specimens with the presence of Nmm-cats turned black during burning, but there was still no formation of protective char layer on the top of specimens. The results listed in Table II show that the LOI values increase slightly with the increase of Nmm-cat amounts in LLDPE matrix. Compared with the significant improvement of flame retardant properties demonstrated by cone experiments for LLDPE/Nmm-cats, the lower enhancement of LOI value is likely due to the difference in outside combustion surroundings between both measure-

ments. The 50 kW/m^2 of the heat flux in cone measurements belong to a forced flaming condition, which provide a crucial heat to keep high carbonization activities of the Nmm-cats.

For investigating the effects of the above Nmm-cats on the flame retardancy of polyolefins with different chemical structures, we replaced LLDPE by PP in the present work. The flame retardancy and the char yield of the resultant PP/Nmm-cats composites are reported in Figure 3 and Table III. After comparing the results for PP/Nmm-cats and LLDPE/Nmm-cats, a parallel trend is observed for the PHRR, THR, average EHC, and char yield. However, it is note-worthy that the PP composites show a higher char yield and better flame retardancy, indicating that the chemical structure of polyolefins also influences the carbon deposition due to the release of different degradation products.

The microstructures of the carbonaceous substances formed from LLDPE/5 wt % Nmm-cats were examined by SEM, TEM and Raman spectra. The SEM studies of the final residues as shown in Figure 4(a,b), which reveal that a major part of the residues have amorphous carbon structure and the other minor parts belong to tube-like nanostructures with diameters ranging from about 40 to 60 nm. TEM studies further confirm that these nanostructures are multiwalled carbon nanotubes (MWNTs) as shown in Figure 4(c). It is not similar with the results in our previous work,²⁷ because the major parts of final residues achieved in our previous work are comprised of the MWNTs. The results of Raman spectra give us more whole

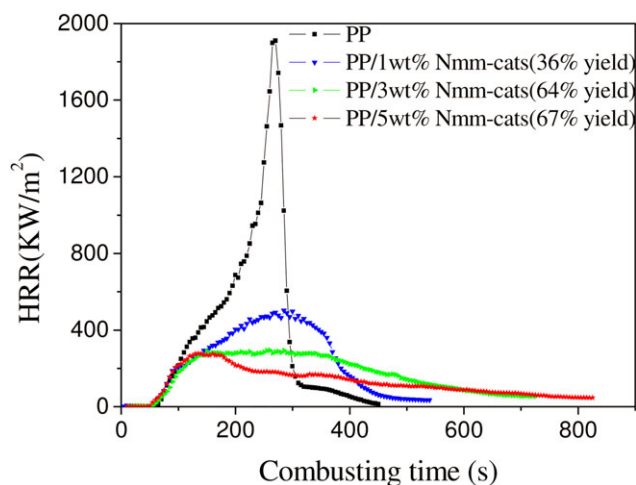


Figure 3. Effects of the mass fraction of Nmm-cats on the heat release rate of PP/Nmm-cats. [Color figure can be viewed in the online issue, which is available at wileyonlinelibrary.com.]

Table III. Cone Calorimeter Data of PP and PP/Nmm-Cat Composites

| Properties | PP | PP/1% Nmm-cat | PP/3% Nmm-cat | PP/5% Nmm-cat |
|---------------------------|------|------------------|------------------|------------------|
| IT(s) | 64 | 62 | 63 | 60 |
| PHRR (kW/m ²) | 1909 | 490 | 292 | 275 |
| THR (MJ/m ²) | 254 | 205 | 168 | 149 |
| Average EHC (MJ/Kg) | 40.5 | 38.7 | 35 | 33 |
| Char yield (%) | 0 | 22.7 | 51 | 58 |

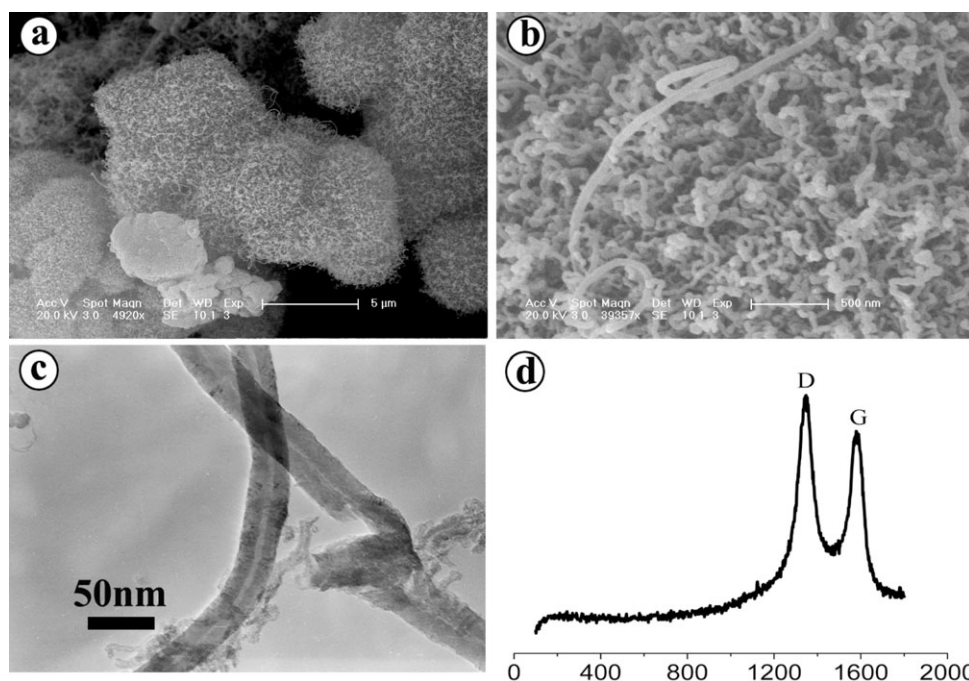


Figure 4. Macrostructures and Raman spectra of carbonaceous substances obtained from LLDPE/5 wt % Nmm-cats.

properties of the final residues. Normally, the D-band at about 1348 cm^{-1} is associated with vibration of carbon atoms with dangling bonds in the plane terminations of disordered graphite, and the peak at 1589 cm^{-1} (G-band) corresponds to an E_{2g} mode of hexagonal graphite and is related to the vibration of sp_2 -bonded carbon atoms in a graphite layer.²⁸ As shown in Figure 4(d), a high ratio of $I_D/I_G = 1.2$ indicates that the major constituent of char belongs to amorphous carbon and the levels of MWNTs in the final composition of the residues are relatively low.

The mechanisms regarding to the very high charring capacity of the Nmm-cats must be commented. As mentioned in the introduction part, the Mo/Mg/ Ni/O metal oxides, as a kind of carbon-forming catalysts, have been applied to produce MWNTs by several authors. A widely accepted mechanism has been proposed that Mg and Mo elements included in Ni catalysts could effectively prolong the catalytic lifetime of catalysts. In the course of MWNT synthesis via a typical CVD device, the controlled hydrocarbon flow continuously passes through the surface of catalysts. In contrast with the MWNT synthesis, the char-forming systems of polyolefins are very unique because the gas-phase degradation products as carbon source are limited and pass quickly from the surface of Nmm-cats. Thus, addressing the effects of Mo and Mg elements on the Ni catalysts in this work seems to be very interesting to study the charring mechanism of the Mo/Mg/ Ni/O catalysts.

The XRD measurements were performed on the charring catalysts and their corresponding final residues from LLDPE for a range of Mo and Mg molar fraction. It is estimated that the low-degree improvement of the char yield by the addition of Mg element probably only attributes to its physical effects on the Ni catalysts. Indeed, the diffraction peaks of Mg/Ni/O with

any Mg molar fractions considered in this work are basically identical with those of Ni/O catalysts, which mean that the Mg element included in the Mg/Ni/O has no effects on the phase structure of Ni/O catalysts under this experimental condition. The same phenomena were also observed for their corresponding final residues. In addition, it is generally accepted that the Mg elements can not carbonize catalytically aliphatic hydrocarbon structures under this condition. Thus, we tentatively conclude that the improvements of char yield by adding Mg

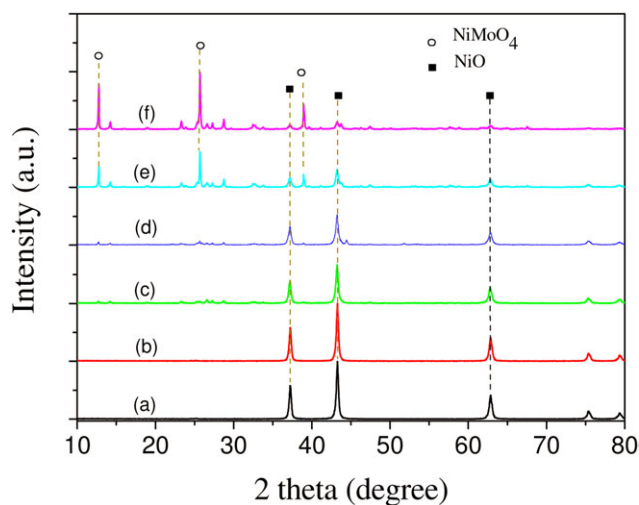


Figure 5. XRD patterns of Nmm-cats with a range of Mo molar fraction: (a) CA3 (Mg/Ni = 1/7), (b) CA8 (Mo/Mg/Ni = 0.21/1/7), (c) CA9 (Mo/Mg/Ni = 0.42/1/7), (d) CA10 (Mo/Mg/Ni = 0.7/1/7), (e) CA11 (Mo/Mg/Ni = 1.05/1/7), and (f) CA12 (Mo/Mg/Ni = 1.4/1/7). [Color figure can be viewed in the online issue, which is available at wileyonlinelibrary.com.]

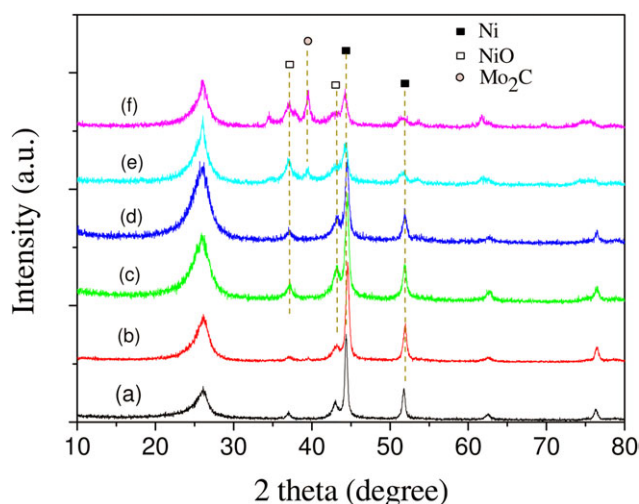


Figure 6. XRD patterns of responding final residues obtained from LLDPE/Nmm-cats with a range of Mo molar fraction: (a) CA3 (Mg/Ni = 1/7), (b) CA8 (Mo/Mg/Ni = 0.21/1/7), (c) CA9 (Mo/Mg/Ni = 0.42/1/7), (d) CA10 (Mo/Mg/Ni = 0.7/1/7), (e) CA11 (Mo/Mg/Ni = 1.05/1/7), and (f) CA12 (Mo/Mg/Ni = 1.4/1/7). [Color figure can be viewed in the online issue, which is available at wileyonlinelibrary.com.]

element appropriately should be attributed to the increase in the utilization ratio of Ni/O catalysts. The decrease of charring yield after a threshold can be attributed to over high levels of the Mg fractions in Nmm-cats, which not only results in the reduction of Ni molar fractions at a fixed amount of catalysts in LLDPE but also probably induces a barrier effect between the degradation products and the surface of Ni catalysts.

Comparatively, the presence of Mo element in Ni catalysts induces a dramatic enhancement in char yield. Figure 5 shows the XRD patterns of a series of catalysts with different Mo molar fractions (Table I), namely CA3 (Mg/Ni = 1/7), CA8 (Mo/Mg/Ni = 0.21/1/7), CA9 (Mo/Mg/Ni = 0.42/1/7), CA10 (Mo/Mg/Ni = 0.7/1/7), CA11 (Mo/Mg/Ni = 1.05/1/7), and CA12 (Mo/Mg/Ni = 1.4/1/7). As for the CA3, only the characteristic diffraction peaks of NiO were observed and no MgO phases were detected in Figure 5(a). With increasing the molar fraction of Mo in the catalysts, however, the XRD patterns show notable changes in Figure 5(b–e), in which the diffraction peaks of NiO become weak and some new diffraction peaks appear due to the formation of NiMoO₃. The contrast with no effects on the Ni characteristic diffraction peaks by the presence of Mg elements indicates that Mo element is much easier to coexist with Ni in a single catalyst particle by the formation of Mo–Ni oxide alloy. We thus expect that there must be some chemical interactions between Mo and Ni elements in the carbonization of the degradation products.

Figure 6 shows the XRD patterns of the corresponding residues of these catalysts for investigating the phase transformation of catalysts after pyrolysis. The CA3 catalysts, as Mg/Ni/O catalysts with the molar ratio of Mg/Ni = 1/7, gave a much lower char yield relative to the Mo-containing catalysts. Figure 6(a) reveals the presence of the NiO phase and the deactivated metallic Ni phase in its final residues. With increasing the molar fraction of

Mo in the catalysts, some new diffraction peaks appear in the XRD patterns of char residues. Especially in Figure 6(e,f), the presence of Mo₂C phase is detected evidently. In the following paragraph, we make a detail analysis on the reason of significant enhancing of the char yield by the appropriate incorporation of Mo element.

Generally, carbon species deposit rapidly on the surface of Ni catalysts owing to the easy-formed nickel carbide (C[sbond]Ni) under high temperature conditions. However the breaking of the thermodynamically unstable C[sbond]Ni often results in the deactivation of Ni catalysts with coating of amorphous carbon on their surfaces. In contrast, the Mo[sbond]C bond is very stable relative to the Ni[sbond]C bond under high temperature conditions. When Mo element is added to the Ni catalysts to form Ni–Mo alloy, the Mo[sbond]C bond will partially replace the Ni[sbond]C bond during carbon formation [Figure 6(b–e)] which finally results in the improvement of char yield. However, it has been demonstrated in Table I that further increasing the molar fraction of Mo in the Mo/Mg/Ni/O catalysts lead to the char yield reduction. We attribute this result to the decrease of Ni molar fractions at a fixed amount of catalysts in LLDPE and the activity reduction of the catalysts due to it needs much higher temperature to form Mo₂C than that of nickel carbide.

CONCLUSIONS

The Nmm-cats with the molar ratio of Mo/Mg/Ni = 0.7/1/7 was successfully prepared as charring catalysts for polyolefins. It could effectively transfer noncharring polyolefins to charring polymers by catalytic carbonization under forced flaming conditions. After pyrolysis in a model charring test, about 56 and 64% of char residues were left from LLDPE/3 wt % Nmm-cats and PP/3 wt % Nmm-cats, respectively. Significant improvement of flame retardancy of LLDPE and PP was demonstrated by the cone calorimeter experiment, whereas the LOI values increased slowly with the presence of Nmm-cats. XRD results indicated that the high charring capacity of the Nmm-cats was credited to the appropriate addition of Mo and Mg elements, where the Mg element improved the utilization ratio of Ni catalysts by physical effects and the Mo element dramatically promoted the catalytic activity by forming more thermal-stable Mo[sbond]C bond. The high carbon-forming effectiveness of the Nmm-cats in this work would not be limited to the LLDPE and PP matrix. We believe that transferring the noncharring polyolefins to charring polymers by depositing most of volatiles as carbonaceous substances during combustion represents a novel nonhalogenated flame retarding approach for the polyolefins.

ACKNOWLEDGMENTS

This work was supported by the Fundamental Research Funds for the Central Universities (DL12DB02).

REFERENCES

1. Eckersley, S. T.; Chaput, A. B. *J. Appl. Polym. Sci.* **2001**, *80*, 2545.

2. Gleixner, G. *Chem Fibers Int.* **2001**, *51*, 422.
3. Mueller, P. A.; Richards, J. R.; Congalidis, J. P. *Macromol. Res.* **2011**, *5*, 261.
4. Guo, X. F.; Kimb, J. H.; Kim, G. J. *Catal. Today* **2011**, *164*, 336.
5. Luo, Y. L.; Chen, Q. Y.; Zhu, D.; Matsuo, M. *J. Appl. Polym. Sci.* **2010**, *116*, 2110.
6. Cokoja, M.; Christian Bruckmeier, D. C.; Rieger, B.; Herrmann, W. A.; Kühn, F. E. *Angew Chem. Int. Ed.* **2001**, *50*, 8510.
7. Takenaka, S.; Shigeta, Y.; Tanabe, E.; Otsuka, K. *J. Phys. Chem. B* **2004**, *108*, 7656.
8. Wang, S. B.; Lu, G. Q. *Energy Fuel* **1998**, *12*, 248.
9. Liu, X. L.; Ly, J.; Han, S.; Zhang, D. H.; Requicha, A.; Thompson, M. E.; Zhou, C. W. *Adv. Mater.* **2005**, *17*, 2727.
10. Atiyah, M. R.; Awang Biak, D. R.; Ahmadun, F.; Ahamad, I. S.; Mohd Yasin, F.; MohamedYusoff, H. *J. Mater. Sci. Technol.* **2011**, *27*, 296.
11. Nikolaev, P.; Bronikowski, M. J.; Bradley, R. K.; Rohmund, F.; Colbert, D. T.; Smith, K. A.; Smalley, R. E. *Chem. Phys. Lett.* **1999**, *313*, 91.
12. Yun, Y. H.; Shanov, V.; Tu, Y.; Subramaniam, S.; Schulz, M. J. *J. Phys. Chem. B* **2006**, *110*, 23920.
13. Hata, K. J.; Futaba, D. N.; Mizuno, K.; Namai, T.; Yumura, M.; Iijima, S. *Science* **2004**, *306*, 1362.
14. Tang, T.; Chen, X. C.; Chen, H.; Meng, X. Y.; Jiang, Z. W.; Bi, W. G. *Chem. Mater.* **2005**, *17*, 2799.
15. Song, R. J.; Jiang, Z. W.; Yu, H. O.; Liu, J.; Zhang, Z. J.; Wang, Q. W.; Tang, T. *Macromol. Rapid Commun.* **2008**, *29*, 789.
16. Yu, H. O.; Zhang, Z. J.; Wang, Z.; Jiang, Z. W.; Liu, J.; Wang, L.; Wan, D.; Tang, T. *J. Phys. Chem. C* **2010**, *114*, 13226.
17. Tang, T.; Chen, X. C.; Meng, X. Y.; Chen, H.; Ding, Y. P. *Angew Chem. Int. Ed.* **2005**, *44*, 1517.
18. Song, R. J.; Jiang, Z. W.; Bi, W. G.; Cheng, W. X.; Lu, J.; Huang, B. T.; Tang, T. *Chem. Eur. J.* **2007**, *13*, 3234.
19. Li, Y.; Zhang, X. B.; Tao, X. Y.; Xu, J. M.; Huang, W. Z.; Luo, J. H.; Luo, Z. Q.; Li, T.; Liu, F.; Bao, Y.; Geise, H. J. *Carbon* **2005**, *43*, 295.
20. Zhou, L. P.; Ohta, K. S.; Kuroda, K.; Lei, N.; Matsuishi, K.; Gao, L. Z.; Matsumoto, T.; Nakamura, J. *J. Phys. Chem. B* **2005**, *109*, 4439.
21. Patil, K. C. *Bull. Mater. Sci.* **1993**, *16*, 533.
22. Gilman, J. W.; Jackson, C. L.; Morgan, A. B.; Harris, R.; Manias, E.; Giannelis, E. P.; Wuthenow, M.; Hilton, D.; Phillips, S. H. *Chem. Mater.* **2000**, *12*, 1866.
23. Fina, A.; Camino, G. *Polym. Adv. Technol.* **2011**, *22*, 1147.
24. Pastore, H. O.; Frache, A.; Boccaleri, E.; Marchese, L.; Camino, G. *Macromol. Mater. Eng.* **2004**, *289*, 783.
25. Schartel, B.; Wei, S. A.; Sturm, H.; Kleemeier, M.; Hartwig, A.; Vogt, C.; Fischer, R. X. *Polym. Adv. Technol.* **2011**, *22*, 1581.
26. Song, R. J.; Wang, Z.; Meng, X. Y.; Zhang, B. Y.; Tang, T. *J. Appl. Polym. Sci.* **2007**, *102*, 5988.
27. Song, R. J.; Ji, Q. *Chem. Lett.* **2011**, *40*, 1110.
28. Sun, Z. Y.; Masa, J.; Liu, Z. M.; Schunhmann, W.; Muhler, M. *Chem. Eur. J.* **2012**, *18*, 6972.